Request ~~DRF~~ CR-

1/69

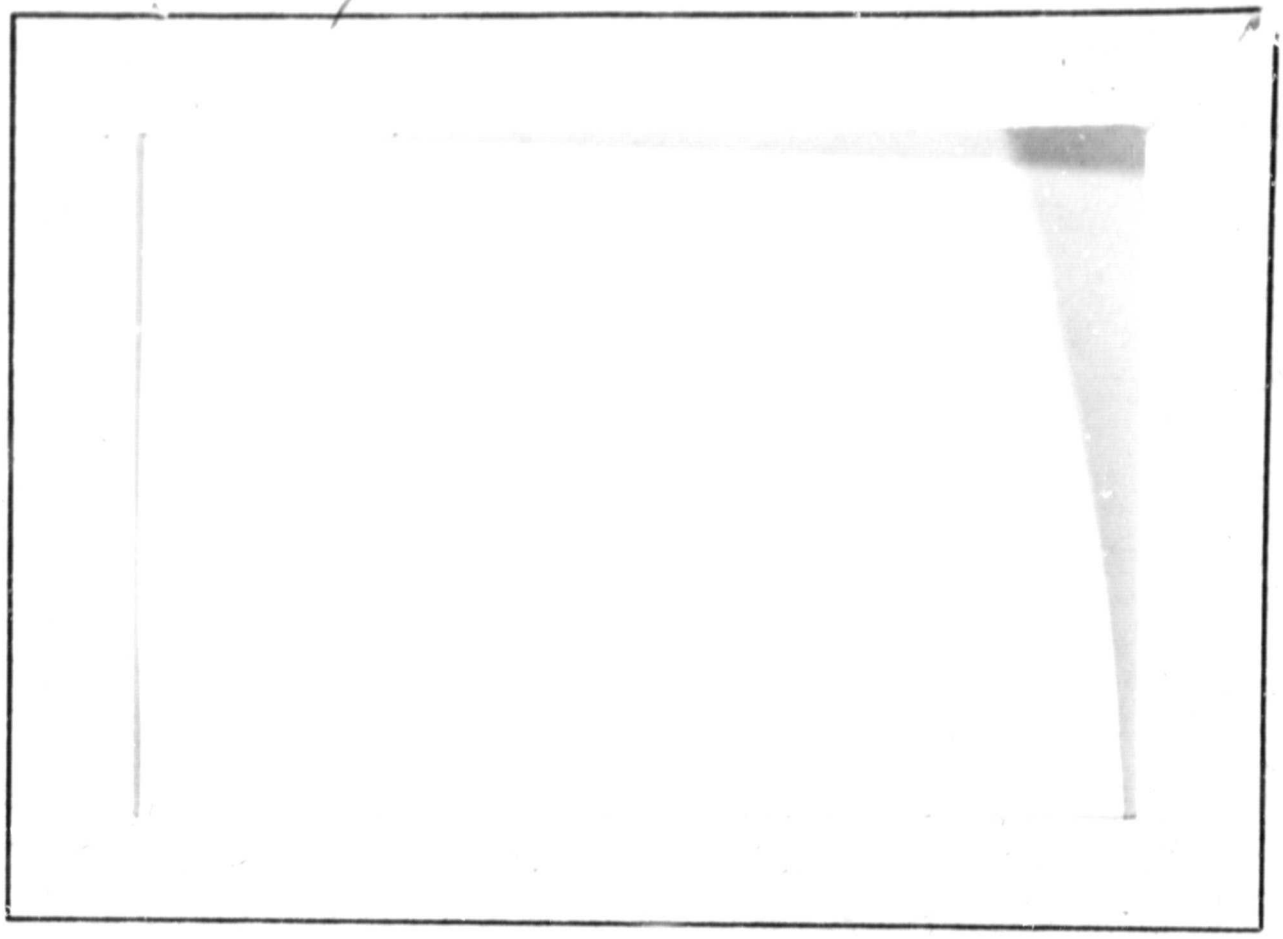

COSMIC RAY GROUP

School of Physics and Astronomy

UNIVERSITY OF MINNESOTA

NGL-24-005-008

Intensity Correlations and Substorm Electron Drift Effects in the Outer Radiation Belt Measured with the OGO-III and ATS-1 Satellites

K. A. Pfitzer and J. R. Winckler

Technical Report

CR-136

April, 1969

School of Physics and Astronomy
University of Minnesota
Minneapolis, Minnesota

Abstract

During late December 1966 and January 1967 the elliptically orbiting satellite OGO-III entered the magnetosphere within 30° of the subsolar point and within 10° of the geomagnetic equator. This permits the measurement of r_b, the distance to the magnetosphere boundary, which is a necessary parameter for the Mead model magnetic field calculations. The electron fluxes measured by an electron spectrometer and an ion chamber on OGO-III are correlated with electron fluxes on the geostationary satellite ATS-1 at the exact time when both satellites are on the same drift shells as calculated from the Mead model magnetic field with separations in local time up to 180°. During quiet times an absolute comparison of the fluxes from 50-1000 keV gives a linear relationship indicating agreement of the measurements over a three order of magnitude range of intensities. During substorm increases the ATS-1 measurements have similar profiles but are delayed in time with respect to each other. The observed delays are smaller for higher energy electrons and larger for greater separations in local time. As an example, the measured delays for 50, 150 and 400 keV electrons on January 11, 1967 when the local time separations was 110° are 26, 13-17 and 5 minutes, respectively. The observed delays are consistent with newly created electrons being produced in a region near local midnight. These newly produced electrons then gradient drift past the two satellites. The production region is shown to be 30° - 60° in width and about 4 earth radii in depth.

1. Introduction

The work described in the following grew out of an attempt to understand the complex variations in the energetic electron intensities in the outer Van Allen belt. That large variations in outer zone electron intensities occur during magnetic storms has been known for more than a decade, and studied by numerous investigators (e.g. see Hess, 1968, Chapters 6 and 10). These variations were clearly evident in the electron spectrometer and ion chamber measurements on the OGO-I and OGO-III satellites (50 keV to 4 meV range (Pfitzer, 1968; Pfitzer and Winckler, 1968; Kane, 1967)) beginning with the last solar minimum in 1964 and extending to the present. However, the infrequent traversals of the belts by the OGO spacecraft (orbital periods of the order of two days) created insurmountable problems for outer zone studies, as important time variations of the electron flux occur in hours or minutes. The geostationary orbit of ATS-1, on the other hand, permits an excellent detailed examination of time variations in the fractional second up to seasonal time scales (Lezniak et al., 1968; Lezniak and Winckler, 1968; Parks and Winckler, 1969), but the orbit covers a very limited region of the magnetosphere. Since both the ATS-1 and the OGO-III satellites have been instrumented with very similar energetic (50-1000 keV) electron spectrometers, the correlation of the two satellites in the outer zone provides the possibility of gaining insight into the space-time distribution of the radiation.

Part 2 below is an exercise designed to test the applicability of known models of the distorted magnetosphere during quiet conditions, and to build confidence that under these known conditions, the spectrometers could be brought into simultaneous agreement at various points on common drift shells in the very slowly changing outer zone. In Part 3 the comparison is extended to cases of large electron flux increases during magnetospheric

substorms typified by auroral zone bay events (Parks et al., 1968; Jelly and Brice, 1967). The time variation of these events and evidence that they represent freshly accelerated particles has been given by ATS-1 results (Lezniak et al., 1968; Parks and Winckler, 1968) as well as by lower altitude polar orbiting vehicles (McDiarmid, 1969; Jelly and Brice, 1967). Recently, Arnoldy (1969) has presented evidence that the characteristic 50 keV electron flux increases of about one hour's duration seen by the ATS-1 spectrometer at all local times are delayed from midnight bays by an amount roughly proportional to the local time, and of the correct magnitude to be interpreted as drift effects. In what follows we have brought the two-satellite technique to bear on this problem and although with fewer cases, have been able to confirm Arnoldy's ideas and to examine the energy dispersion and timing of the events in some detail.

2. Quiet Day Correlations

The ATS-1 satellite which is in geostationary orbit at 6.6 R_e moves slowly with respect to the radiation belts. Since the electron drift shells are approximately circular even in the distorted magnetosphere the satellite moves approximately along a given drift shell while increasing its location in local time 15° per hour.

Since the satellite remains on a given drift shell for an extended period of time it is possible to correlate easily the ATS-1 data with all the passes of the elliptically orbiting satellite (OGO-III) which crosses the drift shells more rapidly. A time can always be found when both ATS-1 and the elliptically orbiting satellite are on the same drift shell and thus a study of the azimuthal dependence of the fluxes on drift shells intersecting the ATS-1 orbit can be made. One must, however, be able to calculate the electron drift shells before a study of the azimuthal

dependence can be successful. Although the McIlwain L parameter as generally used provides a first approximation, it is not very effective for distances greater than 5 R_e. In this paper we have used the Mead model description of the magnetic field (Mead, 1964) for calculating the drift shells. This earlier Mead model uses only the location of the boundary at the subsolar point whereas a later version (Williams and Mead, 1965) depends on both the location of the boundary and the strength of the tail field. We have no data available at present which will give us the strength of the tail field during our period of comparison. We are, however, able to measure the location of the boundary at the subsolar point and therefore the earlier Mead model is used in this analysis.

During late December 1966 and during January 1967, the OGO-III satellite entered the magnetosphere within 30° longitude of the subsolar point and within 10° of the magnetic equator. It was therefore possible to measure the location of the magnetopause within a few hours of the OGO-III and ATS-1 correlation. The boundary crossing as determined by the 50 keV electron flux cutoff is used to determine the input parameter r_b (the distance to the boundary in earth radii) for the Mead model magnetic field calculations. Assuming constancy of the first adiabatic invariant and using the Mead model magnetic field, the drift shell passing through a specified location of ATS-1 is determined for electrons having a pitch angle $\alpha = 90°$. The following procedure is used for determining the time when both ATS-1 and OGO-III are on the same drift shell.

1. A drift shell is determined which passes through the position of the ATS-1 satellite (at local time LT and distance 6.6 R_e) at the time of the OGO-III 6.6 R_e crossing.

2. The exact time t_s at which OGO-III passes through the above calculated drift shell is then noted. This time may differ from the initial time in step 1 by as much as 45 minutes. However, ATS-1 changes its local time by only 12° during 45 minutes, and moves almost parallel to the calculated drift shell and hence a second iteration and calculation of a new drift shell is, in general, not necessary.

3. The time t_s at which OGO-III crosses the calculated drift shell is then also the time when ATS-1 crosses this same drift shell and is the time at which an absolute comparison of fluxes can be made. Figure 1 shows the ATS-1 and OGO-III orbits as well as a sample drift shell for January 19, 1967 when r_b is measured to be 10.5.

The ATS-1 electron spectrometer and the OGO-III electron spectrometer and ion chamber have been calibrated in the laboratory to give absolute intensity measurements. The following comparisons of the instruments in space will not only study the azimuthal electron distribution but also check the accuracy of the laboratory calibrations. Four separate comparisons are possible and will be described below.

The first is the comparison of the 50-120 keV OGO-III electron spectrometer channel and the 50-150 keV ATS-1 electron spectrometer channel. The energy intervals in general overlap but are not the same width and hence a spectrally dependent correction must be made to the measurements. For typical outer zone spectra this correction is less than 10% for the 50-120 keV channel. The ATS-1 and OGO-III fluxes are plotted versus time and the comparison is made at the time t_s when both instruments are on the same drift shell. Figure 2 shows the ATS-1 and OGO-III comparison on a typical quiet day. The OGO-III fluxes show the distribution observed by OGO-III as it moves through the radiation belts in an almost radial direction (see Figure 1). The gradient is very flat for 50-120 keV electrons when

compared with the higher energy channels. The time t_s is indicated by the line labeled "S" in Figure 2. We note in the example that this is the precise time at which the fluxes on OGO-III and ATS-1 are in best agreement. Thirteen such passes were available when OGO-III entered the radiation belt near the subsolar point, near the geomagnetic equator and when the pitch angle of the electrons measured by OGO-III and ATS-1 were almost the same ($60 \leq \alpha \leq 85$). For each of these cases the rates at the time t_s were compared and a correlation plot was generated in which OGO-III fluxes are plotted versus the ATS-1 fluxes (Figure 3). We note the excellent correlation for the 50-150 keV electrons. A best fit straight line has been drawn through the quiet time points (solid circles) which is at the same time, the line of exact absolute agreement of the two instruments. No correction has been made to bring these fluxes into agreement since the spectrally dependent correction is smaller than the uncertainty in drawing the best fit curve. The triangles represent comparisons made during substorms and lead to important results which will be discussed in the next section of the paper.

The second comparison is between the sum of the 120-290 keV and the 290-690 keV channel of the OGO-III spectrometer and the 150-500 keV channel of the ATS-1 spectrometer. For this comparison we find that the difference in the two energy intervals is substantial and therefore the spectral correction is more important. One can estimate the correction by calculating the difference from the typical measured spectrum which has the form $f(E) = E^{-\gamma}$ where γ is generally between 2.5 and 3.0. The ratio D is

$$D = \frac{\int_{120}^{690} f(E)\,dE}{\int_{150}^{500} f(E)\,dE} = \frac{\int_{120}^{690} E^{-\gamma}\,dE}{\int_{150}^{500} E^{-\gamma}\,dE}$$

$D = 1.55$ when $\gamma = 2.5$

$D = 1.66$ when $\gamma = 3.0$

As in the case of the 50-150 keV fluxes, the OGO-III 120-690 keV fluxes are plotted versus the ATS-1 150-500 keV fluxes without applying any corrections to bring the fluxes into agreement. In Figure 4 one finds that as in Figure 3 most of the points fall along a well defined straight line. One finds that there is a systematic discrepancy D' which is

$$D' = \frac{J(120\text{-}690 \text{ keV})}{J(150\text{-}500 \text{ keV})} = 1.9$$

D' is somewhat larger than the calculated correction; however, the agreement between the two instruments after accounting for the correction is better than 15%. In what follows we have used $D' = 1.9$. Once again in Figure 4 points during substorms are indicated by triangles.

The third comparison is between the OGO-III 690-1700 keV electron channel and the ATS-1 500-1000 keV electron channel. This comparison suffers because of poor statistics in the OGO-III measurement and also because of a discrepancy in the energy coverage of the two channels. The correction, D, can again be estimated, and we find $D = .59$ for $\gamma = 2.5$ and $D = .53$ for $\gamma = 3.0$. The correlation plot of Figure 5 shows the discrepancy D' to be 1.2. The scatter of the points makes a comparison of better than 50% impossible.

Because of the poor statistics of the OGO-III 690-1700 keV channel on this shell a fourth comparison has been made. The ion chamber on OGO-III has been shown to be sensitive to electrons above 600 keV (Kane, 1967). This ion chamber, however, is an omnidirectional instrument whereas the ATS-1 spectrometer is directional. But the fluxes near the subsolar point during quiet times at 6.6 R_e have been shown by ATS-1 to be almost isotropic, and therefore dividing the ion chamber rates by 4π will give the approximate

directional flux. Although the absolute electron flux as calculated from the ion chamber is given in Figure 6 it is important to note that one may expect an error of up to a factor of 5 in the electron calibration of the ion chamber when compared with the electron spectrometer on OGO-III (Kane et al., 1967). However, the most important result shown by Figure 6 as well as Figures 3 to 5 is that in all cases the correlation is linear as one would expect unless one of the instruments were to saturate at the highest fluxes, or unless the real magnetic field departs from the Mead model due to distortions which also change the particle fluxes. Figures 3 to 6 show that the electron fluxes at the two satellites are proportional over a three order of magnitude range of intensities, a large range of magnetopause locations ($9.0 \leq r_b \leq 12.5$) as well as a range in local time separations of up to 167°. All the data plotted in Figures 3-6 are contained for reference in Table I.

It was found initially that the comparison of the ATS-1 and OGO-III flux values using the McIlwain L parameter was quite unsuccessful as the scatter of points was large and the intensities measured by the two satellites were not linearly related. This is perhaps as should be expected since the higher fluxes generally correspond to a more distorted magnetosphere and hence a greater error in the McIlwain L parameter. We must conclude that the Mead model gives a good representation of the actual electron drift shells in the quiet-day magnetosphere. This substantiates the result of a somewhat more crucial test described in an accompanying paper (Pfitzer et al., 1969).

3. Substorm Correlations

Since the scatter of points, especially in Figures 3 and 4, is small, the two points (labeled 1 and 30D corresponding to January 1, 1967 and December 30, 1966) which deviate so markedly from the curve aroused considerable

interest. It was found that these two points occurred during substorms as indicated by the presence of a magnetic bay at local midnight. A search of the remainder of the data revealed two other cases in which the correlation time t_s occurred during a substorm. These are on January 11, 1967 and January 15, 1967. Another substorm event was also found on February 8, 1967, but the data was not used for the correlation plots because the OGO-III spectrometer pitch angle is very low ($\alpha = 25°$) and differs from the ATS-1 pitch angle ($\alpha = 80°$) by a large amount.

The comparison of both the 50-150 keV and the 150-500 keV channels on these disturbed days are plotted in detail in Figures 7-11. In these figures the OGO-III 120-690 keV fluxes are divided by 1.9, the ratio determined experimentally by the quiet time correlations. Thus, the effect of the different energy window widths is removed. One should probably at this point refer again to Figure 2, against which the substorm fluctuations in Figures 7-11 can be compared. All of the cases in Figures 7-11 occur during considerable time variations and although in some cases the fluxes agreed at time t_s, we will show below that this was fortuitous. In fact, during disturbed times the Mead model may be only a crude approximation to the actual magnetic field and locating the time t_s becomes very uncertain.

We begin the discussion with Figure 7 which shows the highest flux and the best correlated time variation of the substorm events and occurred on January 11, 1967. If one were to observe the OGO-III spectrometer fluxes without the aid of the ATS-1 correlation, one would probably arrive at the conclusion that OGO-III was observing a storm-time radial distribution. However, the fact that apparently identical distributions are seen by the geostationary ATS-1 satellite which moves very slowly with respect to the radiation belts, suggests that these apparent spatial profiles are

instead explicit time fluctuations. The following observations about the January 11, 1967 event will serve to make clear the exact nature of the time-space relationship of electron fluxes observed by the two spacecraft.

1. The increase in the rates is preceded by a large magnetic bay near local midnight (College) with onset at 1252 UT.

2. The ATS-1 and OGO-III measurements in both channels show a remarkable similarity in their time history although there is a well defined time lag in the OGO-III measurements.

3. During the substorm event observed by ATS-1 at 6.6 R_e, the OGO-III satellite moved from 8.3 R_e to 5 R_e, approximately 3 earth radii; but in spite of this radial motion the profiles were similar.

4. The increase for the 50-150 keV channel is first observed by ATS-1 (LT = 55°) at 1254 UT and by OGO-III (LT = 165°) at 1307 UT, a time lag of 13 minutes.

5. The increase for the 150-500 keV channel is first observed by ATS-1 at 1253 and by OGO-III at 1258, a time lag of 5 minutes.

6. The peak flux for the 50-150 keV channel is observed at 1301 UT by ATS-1 and 1327 UT by OGO-III, a time delay of 26 minutes.

7. The peak flux for the 150-500 keV channel is observed at 1256 UT by ATS-1 and at 1313 UT by OGO-III, a delay of 17 minutes.

Thus:

8. The time lag of the onset and of the flux maxima are energy dependent.

9. The rise time of the event is more rapid for ATS-1 than for OGO-III.

Using the above observations we arrive at the following conclusions: Coincident with a magnetic bay observed at local midnight electrons of energy in the range 50-500 keV appear in the radiation belts in a region near local midnight. This production region is at least 3-4 earth radii in depth

and perhaps 30°-60° in width and continues to produce electrons for about one hour. These newly created electrons begin to gradient drift in the earth's magnetic field and are first observed by the ATS-1 satellite close to midnight. Since the gradient drift speed is dependent on energy, the higher energy electrons which have a higher drift velocity will arrive first at a specified local time. This energy dispersion gives rise to the energy dependent lag times and to the different rise times observed by satellites located at different local times.

At this point, in order to obtain a clearer understanding of the drift phenomena a computer study was employed. A typical substorm observed on the ground as a negative bay and at ATS-1 as a large increase in the 50-500 keV electron flux near local midnight was assumed to be a source of new particles. The prestorm spectrum was assumed to remain fixed and the increases in the rate of the three energy channels were assumed to be due to the addition of these newly accelerated electrons. Figure 12 indicates the initial pre-substorm spectrum, the final spectrum at the substorm maximum and the difference between the two spectra at local midnight. The substorm lasts about an hour, the fluxes rapidly rise to a maximum in about 5-10 minutes, have a rather broad peak and then decay to zero. The computer program traces the drift of each electron on its drift shell, at the drift speed consistent with its energy, in a dipole field, free of electric fields or time variations. The program then calculates the count rate of a given detector having a specified energy response situated at some local time. Figure 13 shows the computer calculated rate versus time history of the 50-150 keV and 150-500 keV electron channels at local times of LT = 0°, 90° and 180°. Prior to the time necessary for one complete revolution around the earth, the time profile at LT = 0° is the profile of the source. About 60 minutes after onset, the 150 keV electrons which were injected at times t = 0 will have been able to complete

one circuit around the earth and will start to contribute to the count rate of the 50-150 keV channel (the dashed line in Figure 13 continues to show the input profile). The higher energy electrons in the 150-500 keV channel have a much greater drift speed and electrons which have made one or more revolutions contribute to the count rate at LT = 0° long before the source decays. The input pulse shape is thus not observable in this energy channel (although the dashed curve indicates the input pulse shape in the figure). At LT = 90° and LT = 180° there is an initial delay before the increase is observed. The increase is first seen in the 150-500 keV channel and then in the 50-150 keV channel. Furthermore, for greater local times the slope of the initial rise is less because of the larger energy dispersion. Because of the steep injection spectrum the 400-500 keV electrons do not contribute significantly to the count rate of the 150-500 keV energy channel and thus the first noticeable increase in the 150-500 keV energy channel corresponds to the arrival of approximately 400 keV electrons, i.e. below the upper edge of the window. This admittedly over-simplified representation of the real dynamic magnetosphere has neglected electric fields, time fluctuations of the magnetic field, all non-dipole effects, various types of diffusion and loss mechanisms, the finite spatial extent of the source, and undoubtedly numerous other complications.

Using the above computer study we now propose that when the 150-500 keV electron channel on ATS-1 and OGO-III first shows an increase it corresponds to the arrival of the 400 keV electrons, and when the peak is reached the 150 keV electrons finally arrive. Similarly for the 50-150 keV energy channel the initial increase corresponds to the arrival of the 150 keV electrons and the maximum corresponds to the arrival of the 50 keV electrons. The theoretical times required for the electrons to drift 110° (the separation of

ATS-1 and OGO-III in local time) is 6, 15 and 34 minutes, respectively for 400, 150 and 50 keV electrons which agrees approximately with the delays between the OGO-III and ATS-1 measurements of 5, 13-17 and 26 minutes. Furthermore, if the onset of the magnetic bay indicates the start of the event, an extrapolation backwards in time shows that the source must be located at approximately 0100 hours local time.

Having discussed the azimuthal drift we now study the other four substorm associated events. Figures 7-11 represent all of the currently available events for the period December 1966 to August 1967 observed by both satellites. The events in Figures 8-11 are not nearly as large or as well defined as the January 11, 1967 event (Figure 7); however, their general behavior will tend to reinforce our conclusions. The December 30th event (Figure 8) shows a small substorm at ATS-1 in the 50-150 keV energy channel at 1030 UT and OGO-III shows a statistically significant peak at 1130 UT. The observed separation in time is about 1 hour, which is the approximate drift time for 50 keV electrons corresponding to the actual difference in local time of the satellites of 167°. The higher energy channel shows an increase at ATS-1 but nothing for OGO-III.

The January 1, 1967 event (Figure 9) is quite complex; however there is an indication that the dip as seen by ATS-1 at 1030 UT which is followed by a sharp rise is reflected by the dip at 1055 UT and the not quite so sharp rise seen by OGO-III. Once again the delay times are approximately consistent with drift period.

The January 15, 1967 event (Figure 10) is quite small in amplitude and not very well defined by OGO-III; nevertheless, we suggest that the peak seen by ATS-1 at 1410 UT is reflected in the rather flat peak observed by OGO-III at 1450 UT.

The February 8, 1967 event (Figure 11) is very complex in structure showing several bays near the shell crossing time. It is, however, the only event when OGO-III is closer to the source than ATS-1. OGO-III (LT = 141°) shows a rather well defined increase starting at 2216 UT and ATS-1 (LT = 186°) shows a rather broad slow increase starting at about 2230 UT. Thus, in this case although the relative position of the two satellites in local time was reversed, the spacecraft closer to midnight detected the event first. We must keep in mind that for this event the OGO-III pitch angle is 25°; whereas, the ATS-1 pitch angle is 80° and hence the fluxes cannot be compared on an absolute level. We show on Figures 7-11 the time t_s for quiet day drift shell coincidence of the two satellites. One can see that agreement of fluxes at t_s in a given channel may be entirely due to chance during these disturbed times (e.g. Figure 7).

Figure 14 has been prepared as a summary of the substorm increases. The flux value prior to the initial increase is used as the base line and a straight line is drawn from the approximate onset to the maximum. We note that whenever both ATS-1 and OGO-III data are available the slope of the measurement having the larger local time is always less and the amplitude always smaller. We also note the general trend of a smaller slope for the larger local times and larger delay times for greater separations in local time.

The above observed delays and changes in slope cannot be due to the relative radial separation or the relative motion of ATS-1 and OGO-III because during two of the events (January 1, 1967 and January 11, 1967) OGO-III was outside the ATS-1 drift shell and moving inwards toward it and during two of the events (December 30, 1966 and January 11, 1967) OGO-III was inside the drift shell and moving inwards away from it.

The only conclusion consistent with the above observations (delays which are dependent on energy and local time separation) is that the measured increases are due to newly accelerated electrons produced in a localized

region of the magnetosphere which then gradient drift past the location of the two satellites. Furthermore, since all of the events are associated with magnetic bays, since it is well known that electrons are injected coincident with the bays (Lezniak et al., 1968; McDiarmid et al., 1969; Parks and Winckler, 1968) and since the time lag between the onset of the bay and the arrival of the electrons tends to zero when the measurement is made closer to local midnight, we must conclude that the observed electrons are injected near local midnight. Arnoldy (1969) has also observed that the delays between magnetic bays near local midnight and ATS-1 electron fluxes are a function of local time and indicate that the delays go to zero near local midnight.

Since the observed delays with respect to the onset of the bay goes to zero as the local time approaches local midnight the source must be located near local midnight. Furthermore, in the substorm comparisons the OGO-III location while observing the substorm fluctuations varied from about 8.5 R_e to 5.2 R_e. Therefore, we conclude that the radial extent of the source region must be at least from 5.2 R_e to 8.5 R_e.

4. Discussion

The application of the two-satellite technique to the outer radiation belt studies of electrons has certain clear advantages. This is particularly true in the present case where both satellites are close to the equatorial plane, are moving rather slowly and measure the same type of particles in the same pitch angle range with calibrated spectrometers giving reasonably energy selection. It is thus not necessary to use associated geophysical phenomena such as bays or riometer absorption events whose exact temporal connection with the trapped radiation is often difficult to establish.

The conclusions that all of the substorm events studied herein show evidence for drifting clouds of electrons starting near the midnight sector differ

from those of other recent investigators including Jelly and Brice (1967), Parks and Winckler (1968) and McDiarmid et al. (1969). In all of these three papers a very extended source was inferred particularly in the paper of McDiarmid in which the source is shown diagramatically stretching from midnight to noon during a substorm. We first make the observation that the presence of precipitation at a given local time, although indicative of a strong perturbation mechanism which is depleting the trapped electrons, is nevertheless not in contradiction to the major source of these trapped particles being near the midnight sector. We know of no reason why a drifting cloud containing a relatively high intensity flux of newly produced electrons should not precipitate continuously as it moves around in local time. One has thus the concept of a "drifting rain cloud" rather than a "leaky bucket" or "splash catcher" model of the radiation. Precipitation from a drifting cloud was suggested and searched for by Jelly and Brice (1967) but with inconclusive results. The loss of electrons from a drifting cloud is quite consistent with a decrease of intensity observed in this paper as local time increases which was also shown earlier in the paper of Lezniak et al. (1968). Such precipitation may be initiated by the wave-particle instability mechanism of Kennel and Petschek (1966) or by fluctuations inherent in the magnetosphere at least throughout the morning hours.

The recent conclusions about the source size of McDiarmid et al. (1969) were based on time comparisons of bay associated electron increases detected by the low altitude polar orbiting satellite, Alouette. It is our opinion that the effects described in the present paper would have escaped notice in the Alouette measurements because of the limited ability of such a satellite to measure accurately the initial time profile of the bay associated increases.

Although it is possible that the "drifting rain cloud" concept may be an important mechanism by which energetic electrons are produced and distributed into the outer zone, certainly the electrons in the outer radiation belt are affected and perhaps owe their origin to a wide variety of processes, some of stochastic nature, others associated with all of the complex sudden changes associated with the solar wind, etc. The substorm increases seem more distinct than other changes because of their association with the auroral bay and electrojet phenomena, and because the effects are large enough and sudden enough to make the injected cloud detectable on its first circuit around the magnetosphere. Details of the substorm-associated magnetospheric motions and a possible generation mechanism for these drifting clouds are discussed in a related paper (Lezniak and Winckler, 1969).

Finally, the definition of the "source size" as given in this paper is certainly only a crude estimate based on a few events. The computer model which was used to help visualize the drift process is much oversimplified compared to the real magnetosphere. Thus the exact boundary of the source in the region of increasing local times away from midnight may be difficult to define and may depend on the degree of the disturbance of the magnetosphere and other factors.

Acknowledgments

We are indebted to George K. Parks and Roger L. Arnoldy for valuable discussions and to Thomas W. Lezniak for special runs of ATS-1 electron spectrometer data. This data study resulting from the ATS-1 and OGO programs is supported by the National Aeronautics and Space Administration under Grant NGL-24-005-008.

TABLE I

Date	t_s	n_b	Local Time		R*	ATS-I FLUXES			OGO-III FLUXES			
			ATS	OGO		50-150 keV	150-500 keV	500-1000 keV	50-120 keV	120-600 keV	600-1700 keV	>1700 keV
30 Dec 66†	1035	10.8	9°	176°	7.0	4.4×10^{6}	9.6×10^{5}	1.5×10^{6}	1.4×10^{6}	1.1×10^{6}	1.0×10^{5}	4.2×10^{4}
1 Jan 67†	1054	10.0	13°	173°	7.3	1.6×10^{6}	1.7×10^{5}	3.2×10^{4}	6.1×10^{5}	3.5×10^{5}	1.3×10^{5}	1.1×10^{4}
5 Jan 67	1208	11.5	32°	168°	7.0	9.0×10^{5}	6.3×10^{5}	8.4×10^{4}	9.4×10^{5}	7.8×10^{5}	1.0×10^{4}	9.6×10^{3}
7 Jan 67	1223	9.0	36°	165°	7.5	3.6×10^{5}	1.6×10^{4}	2.2×10^{3}	5.0×10^{5}	5.4×10^{4}	1.2×10^{4}	3.0×10^{2}
9 Jan 67	1315	11.0	49°	165°	7.0	3.8×10^{6}	8.5×10^{5}	2.6×10^{4}	3.6×10^{6}	---	---	---
11 Jan 67†	1347	11.0	57°	165°	7.0	1.4×10^{7}	1.3×10^{6}	6.2×10^{4}	1.3×10^{7}	1.4×10^{6}	2.3×10^{4}	1.1×10^{4}
15 Jan 67†	1503	12.5	76°	160°	6.7	2.9×10^{6}	1.7×10^{6}	1.2×10^{5}	2.9×10^{6}	3.2×10^{5}	1.5×10^{4}	1.4×10^{3}
17 Jan 67	1536	12.5	84°	160°	6.7	1.8×10^{5}	1.1×10^{6}	2.6×10^{5}	1.8×10^{6}	2.1×10^{6}	$.6\times10^{5}$	5.8×10^{4}
19 Jan 67	1559	10.5	90°	150°	6.9	1.6×10^{6}	5.4×10^{5}	1.5×10^{5}	1.9×10^{6}	1.0×10^{6}	$.3\times10^{5}$	3.1×10^{4}
21 Jan 67	1644	11.0	101°	150°	6.7	5.5×10^{6}	6.5×10^{5}	4.0×10^{4}	5.5×10^{6}	1.4×10^{5}	4.2×10^{4}	5.5×10^{3}
23 Jan 67	1719	12.0	110°	150°	6.7	9.9×10^{5}	4.1×10^{5}	3.4×10^{4}	9.9×10^{5}	7.3×10^{5}	1.5×10^{4}	4.1×10^{3}
25 Jan 67	1754	10.0	119°	150°	6.7	6.3×10^{5}	1.4×10^{5}	1.7×10^{4}	5.0×10^{5}	---	---	2.2×10^{3}
27 Jan 67	1829	10.0	127°	150°	6.7	5.6×10^{5}	1.0×10^{5}	1.6×10^{4}	5.5×10^{5}	2.3×10^{5}	---	2.3×10^{3}
2 Feb 67†	2226	10.0	186°	141°	6.6	3.3×10^{6}	1.1×10^{6}	4.9×10^{4}	1.4×10^{6}	7.6×10^{5}	2.1×10^{5}	1.4×10^{4}

* R is the radial equatorial distance where the common drift shell intersects the OGO-III orbit.

† Substorm events.

Figure Captions

Figure 1: A sample of a drift shell calculated using the Mead model magnetic field and the ATS-1 and OGO-III orbits showing the simultaneous crossing of the drift shell. The OGO-III orbit is projected into the equatorial plane.

Figure 2: Sample quiet time fluxes for ATS-1 and OGO-III showing typical OGO-III radial distributions. The line marked "S" indicates the time t_s when the two satellites are on a common drift shell.

Figure 3: Absolute comparison of the 50-120 keV OGO-III electron channel and the 50-150 keV ATS-1 electron channel. The solid circles indicate comparisons made during quiet times and the triangles represent comparisons made during substorms. The numbers next to the data points indicate the day in January, 1967 when the data was obtained. 30D refers to 30 December, 1966. (Refer to Table I.)

Figure 4: Absolute comparison of the 120-690 keV OGO-III electron channel and the 150-500 keV ATS-1 electron channel. The solid circles indicate comparisons made during quiet times and the triangles represent comparisons made during substorms. The numbers next to the data points indicate the day in January, 1967 when the data was obtained. 30D refers to 30 December, 1966. (Refer to Table I.)

Figure 5: Absolute comparison of the 690-1700 keV OGO-III electron channel and the 500-1000 keV ATS-1 electron channel. The solid circles indicate comparisons made during quiet times and the triangles represent comparisons made during substorms. The numbers next to the data points indicate the day in January, 1967 when the

data was obtained. 30D refers to 30 December, 1966. (Refer to Table I.)

Figure 6: Absolute comparison of the electron fluxes calculated from the OGO-III ionization chamber (sensitive to electrons above 600 keV) with the 500-1000 keV ATS-1 electron channel. The solid circles indicate comparisons made during quiet times and the triangles indicate comparisons during substorms. The numbers next to the data points indicate the day in January, 1967 when the data was obtained. 30D refers to 30 December, 1966. (Refer to Table I.)

Figure 7: ATS-1 and OGO-III 50-150 keV and 150-500 keV electron fluxes for the January 11, 1967 substorm. The line labeled "S" represents the time t_s when the two satellites are on the same drift shell. The small insert represents the relative positions of ATS-1 and OGO-III.

Figure 8: ATS-1 and OGO-III 50-150 keV and 150-500 keV electron fluxes for the December 30, 1966 substorm. The line labeled "S" represents the time t_s when the two satellites are on the same drift shell. The small insert represents the relative positions of ATS-1 and OGO-III.

Figure 9: ATS-1 and OGO-III 50-150 keV and 150-500 keV electron fluxes for the January 1, 1967 substorm. The line labeled "S" represents the time t_s when the two satellites are on the same drift shell. The small insert represents the relative positions of ATS-1 and OGO-III.

Figure 10: ATS-1 and OGO-III 50-150 keV electron fluxes for the January 15, 1967 substorm. The line labeled "S" represents

the time t_s when the two satellites are on the same drift shell. The small insert represents the relative positions of ATS-1 and OGO-III.

Figure 11: ATS-1 and OGO-III 50-150 keV and 150-500 keV electron fluxes for the February 8, 1967 substorm. The line labeled "S" represents the time when both satellites are on the same drift shell. The small insert represents the relative position of ATS-1 and OGO-III. For this event the OGO-III pitch angle is 25° and the ATS-1 pitch angle is 80°.

Figure 12: Typical assumed differential spectrum at local midnight prior to the start of a substorm, at substorm maximum and the difference in the spectrum between the substorm and prestorm.

Figure 12: Computer calculated rate at local time of 0°, 90° and 180° due to the injection of fresh electrons at local midnight. The dashed curves give the input pulse shape at LT = 0.

Figure 14: Composite diagram showing the magnetic bays, the onset times, slopes and amplitudes of the five substorm events.

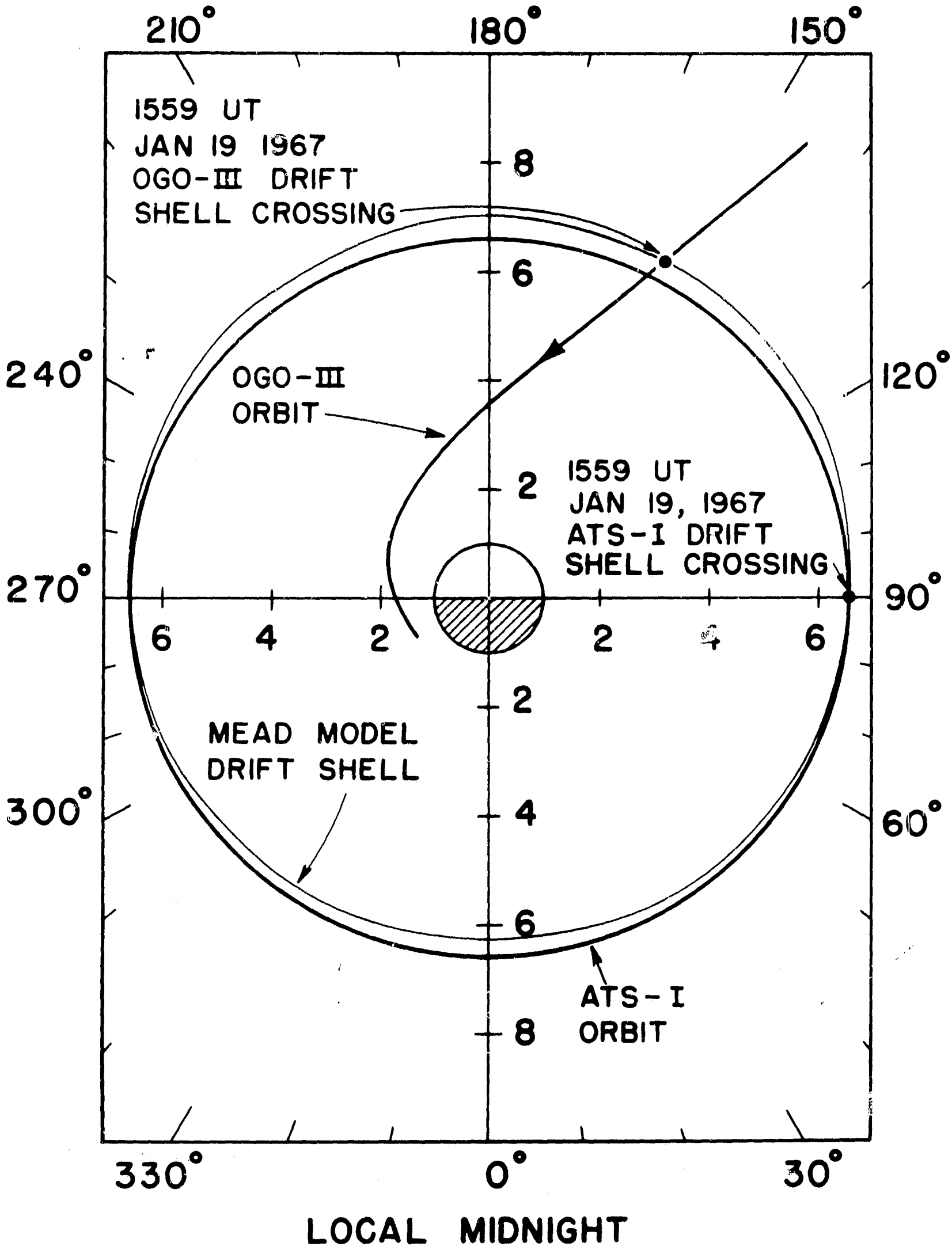
LOCAL NOON
210°
180°
150°
1559 UT
JAN 19 1967
OGO-III DRIFT
SHELL CROSSING
8
6
240°
OGO-III
ORBIT
120°
2
1559 UT
JAN 19, 1967
ATS-I DRIFT
SHELL CROSSING
270°
90°
6 4 2
2 4 6
2
MEAD MODEL
DRIFT SHELL
300°
4
60°
6
ATS-I
ORBIT
8
330°
0°
30°
LOCAL MIDNIGHT

Figure 1

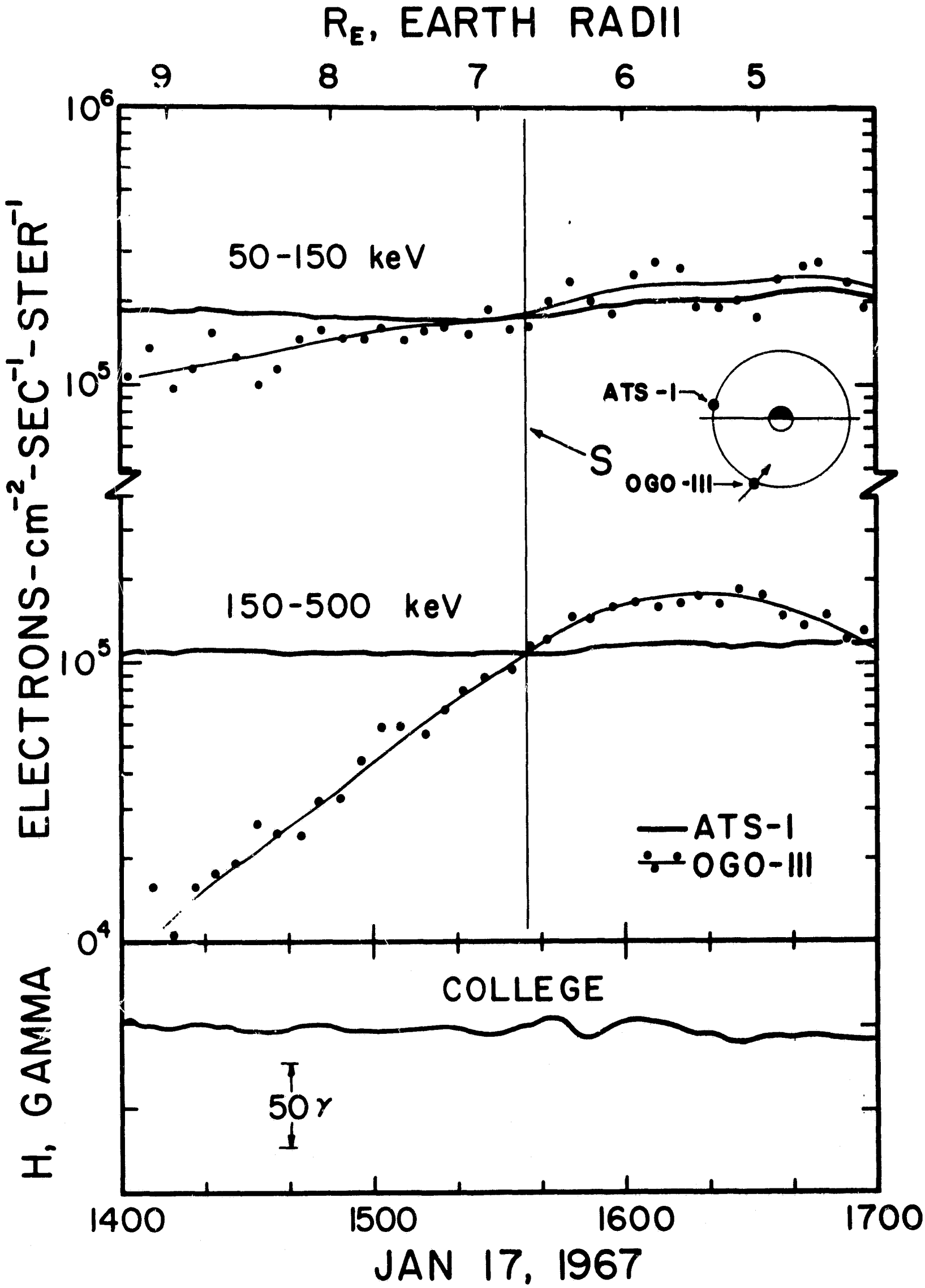
R_E, EARTH RADII
9
8
7
6
5
10^6
10^5
10^4
50-150 keV
150-500 keV
ATS-I
OGO-III
S
ATS-I
OGO-III
COLLEGE
50γ
ELECTRONS-CM^{-2}-SEC^{-1}-STER^{-1}
H, GAMMA
1400
1500
1600
1700
JAN 17, 1967

Figure 2

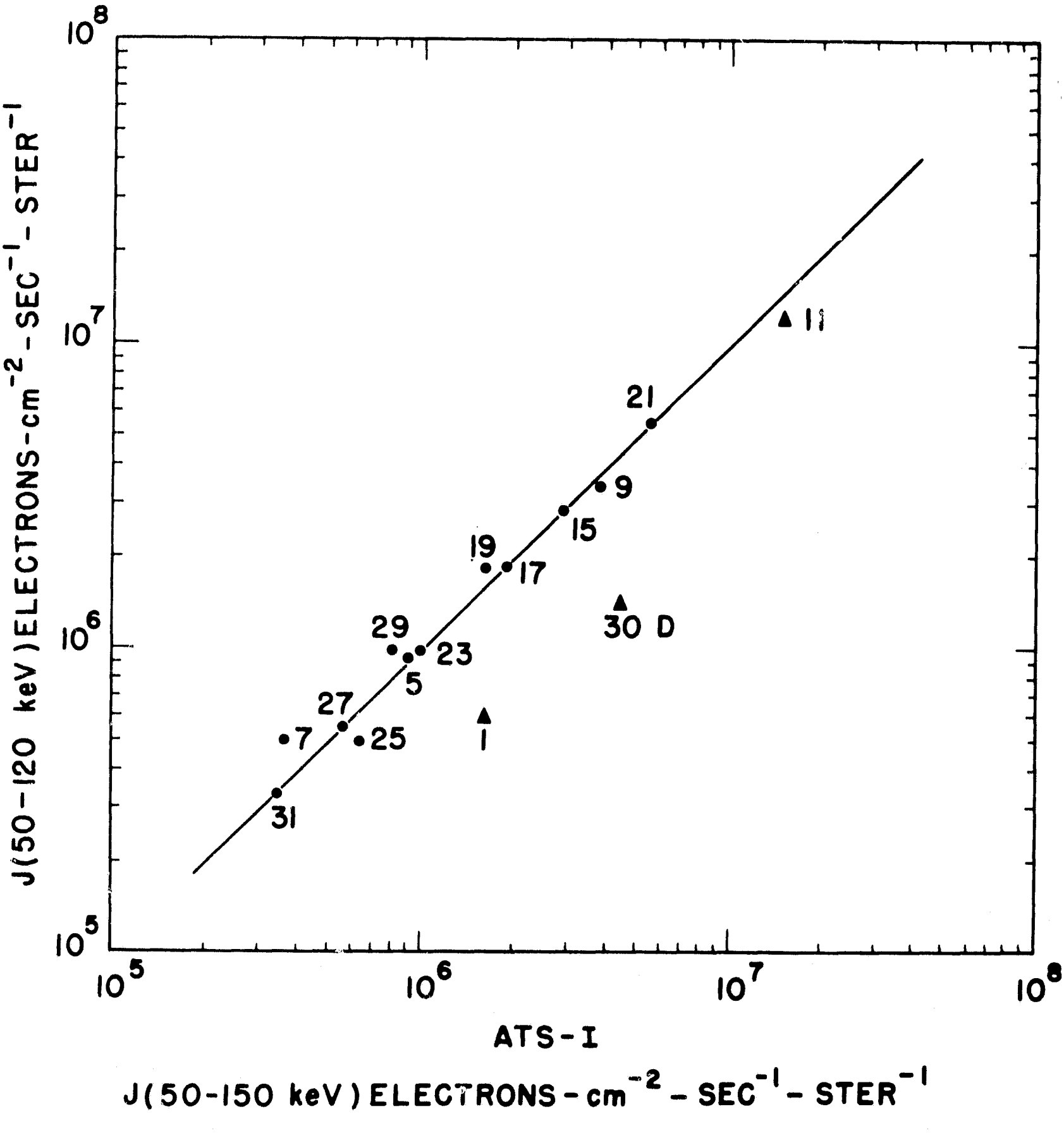
10^8
10^7
10^6
10^5
10^5
10^6
10^7
10^8
J(50-120 keV)ELECTRONS-cm^{-2}-SEC^{-1}-STER^{-1}
ATS-I
J(50-150 keV)ELECTRONS-cm^{-2}-SEC^{-1}-STER^{-1}
11
21
9
15
19
17
30 D
29
23
5
27
7
25
1
31

Figure 3

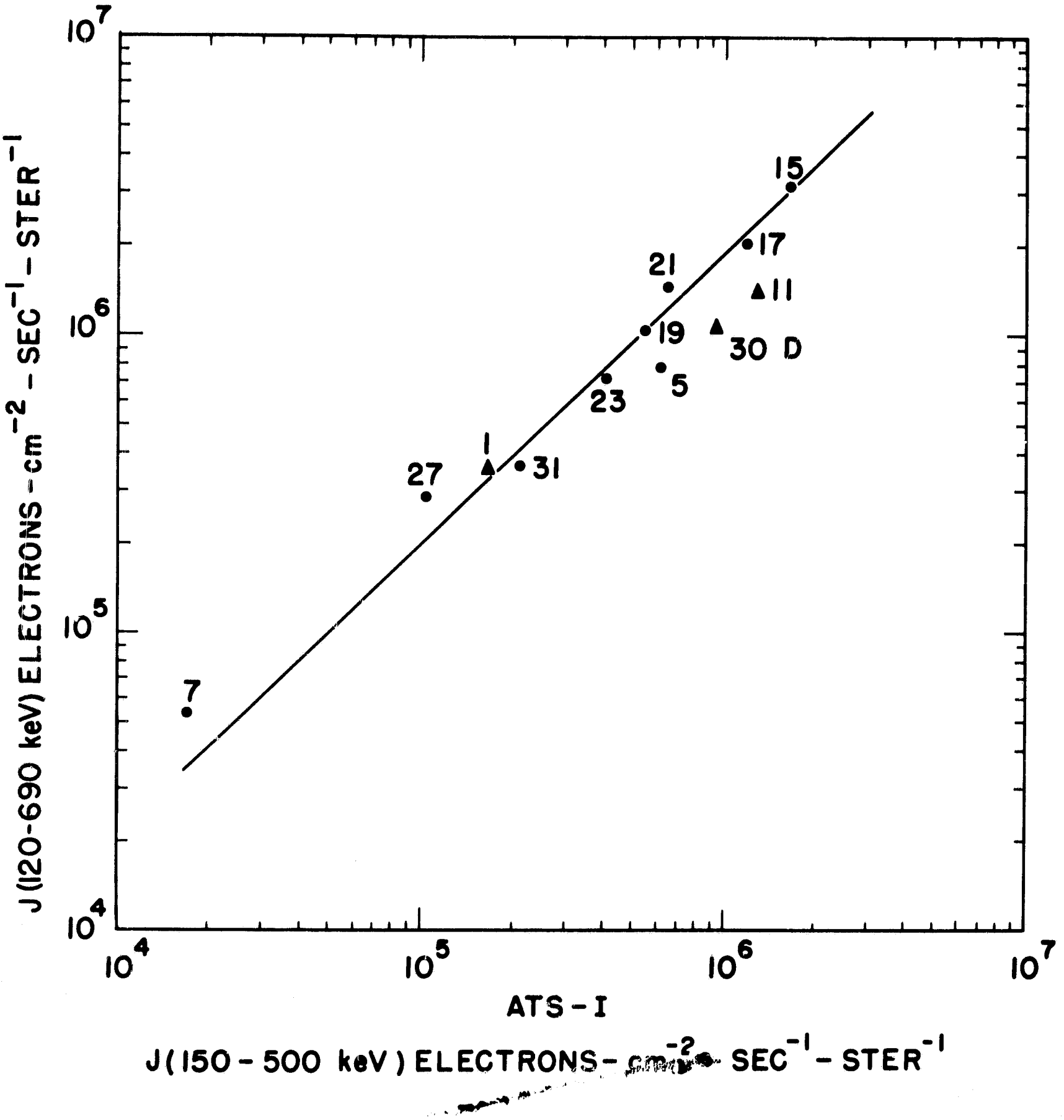
OGO - III
J(120-690 keV) ELECTRONS - cm^{-2} - SEC^{-1} - STER^{-1}
10^7
10^6
10^5
10^4
15
17
21
11
19
30 D
23
5
1
31
27
7
10^4
10^5
10^6
10^7
ATS - I
J(150 - 500 keV) ELECTRONS - cm^{-2} - SEC^{-1} - STER^{-1}

Figure 4

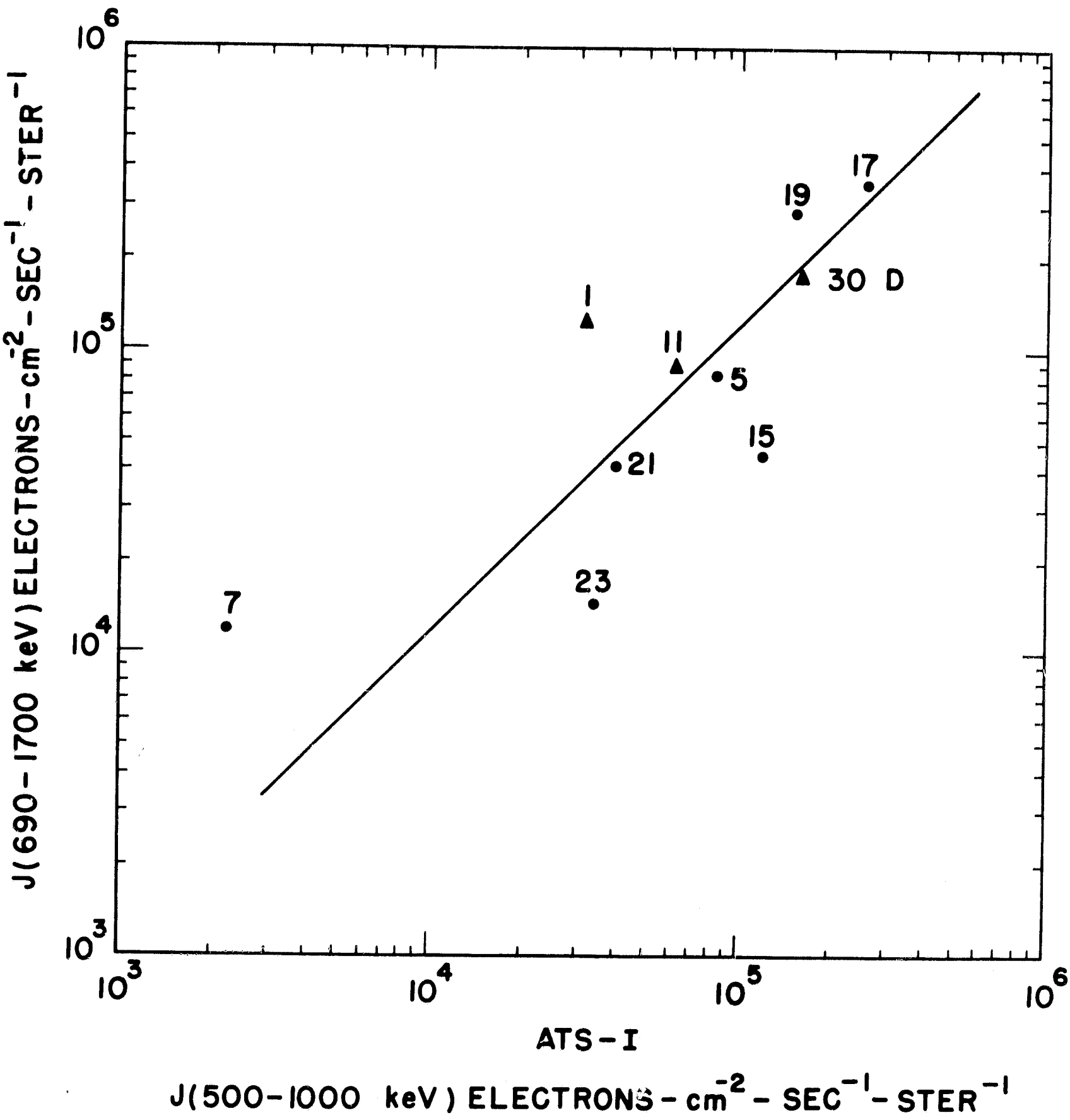
10^6
10^5
10^4
10^3
10^3
10^4
10^5
10^6
J(690-1700 keV) ELECTRONS - cm^{-2} - SEC^{-1} - $STER^{-1}$
ATS-I
J(500-1000 keV) ELECTRONS - cm^{-2} - SEC^{-1} - $STER^{-1}$
1
11
5
15
21
7
23
19
17
30 D

Figure 5

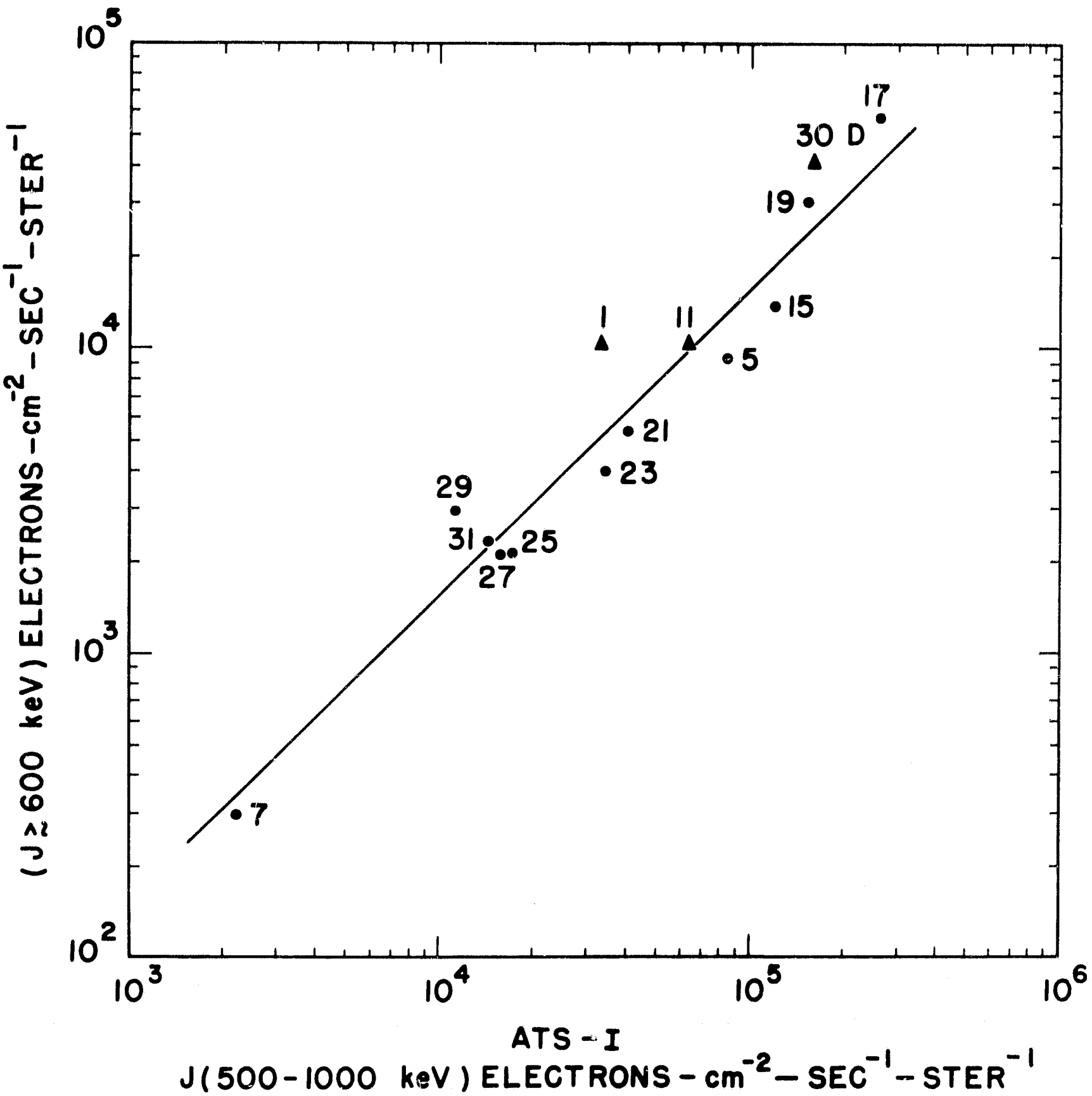
10^5
10^4
10^3
10^2
10^3
10^4
10^5
10^6
17
30 D
19
1
11
15
5
21
23
29
31
25
27
7
OGO-III
(J ≥ 600 keV) ELECTRONS - cm^-2 - SEC^-1 - STER^-1
ATS - I
J(500 - 1000 keV) ELECTRONS - cm^-2 - SEC^-1 - STER^-1

Figure 6

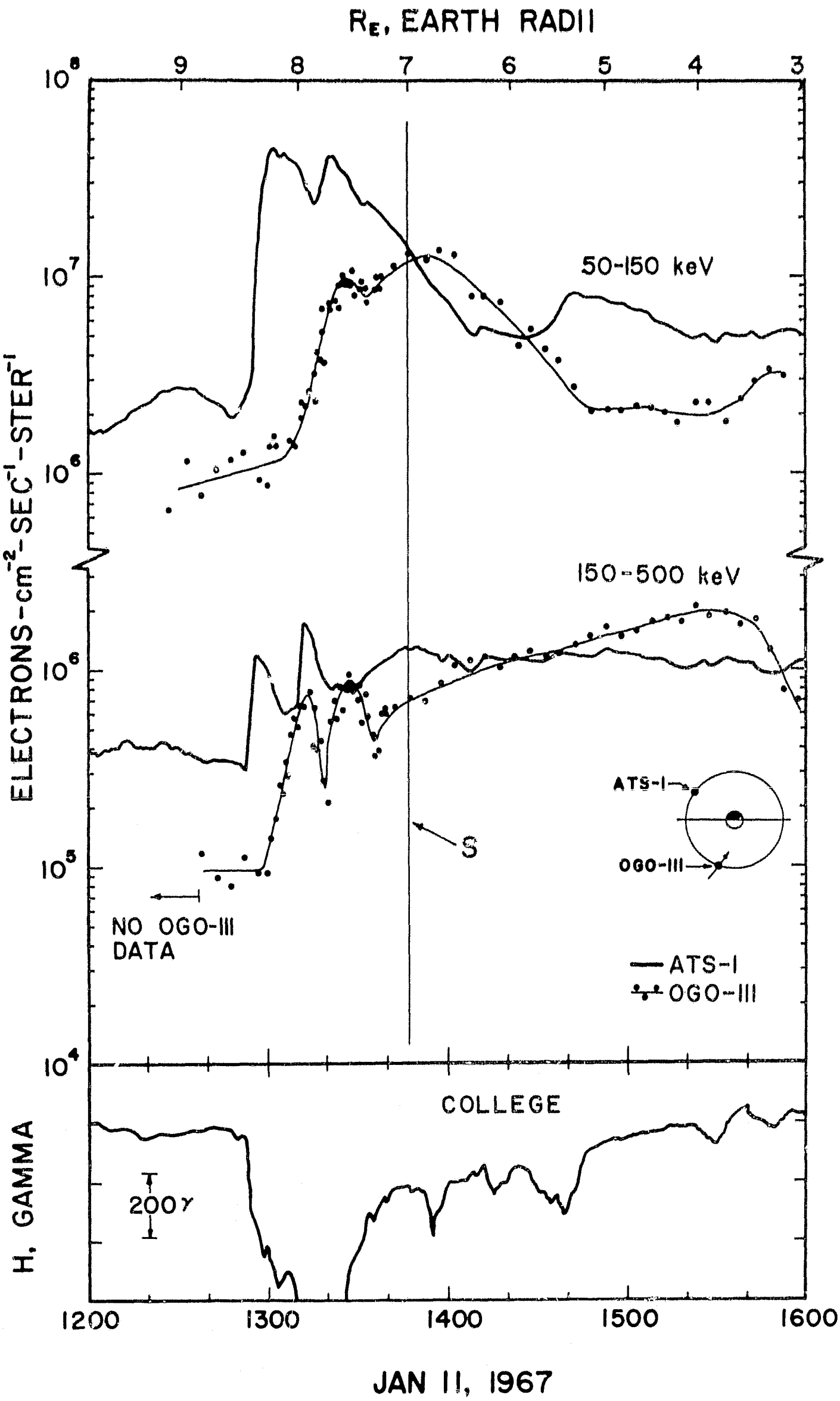
R_E, EARTH RADII
9
8
7
6
5
4
3
10^8
10^7
10^6
10^5
10^4
ELECTRONS-cm^-2-SEC^-1-STER^-1
50-150 keV
150-500 keV
ATS-I
OGO-III
S
NO OGO-III DATA
ATS-I
OGO-III
COLLEGE
H, GAMMA
200γ
1200
1300
1400
1500
1600
JAN 11, 1967

Figure 7

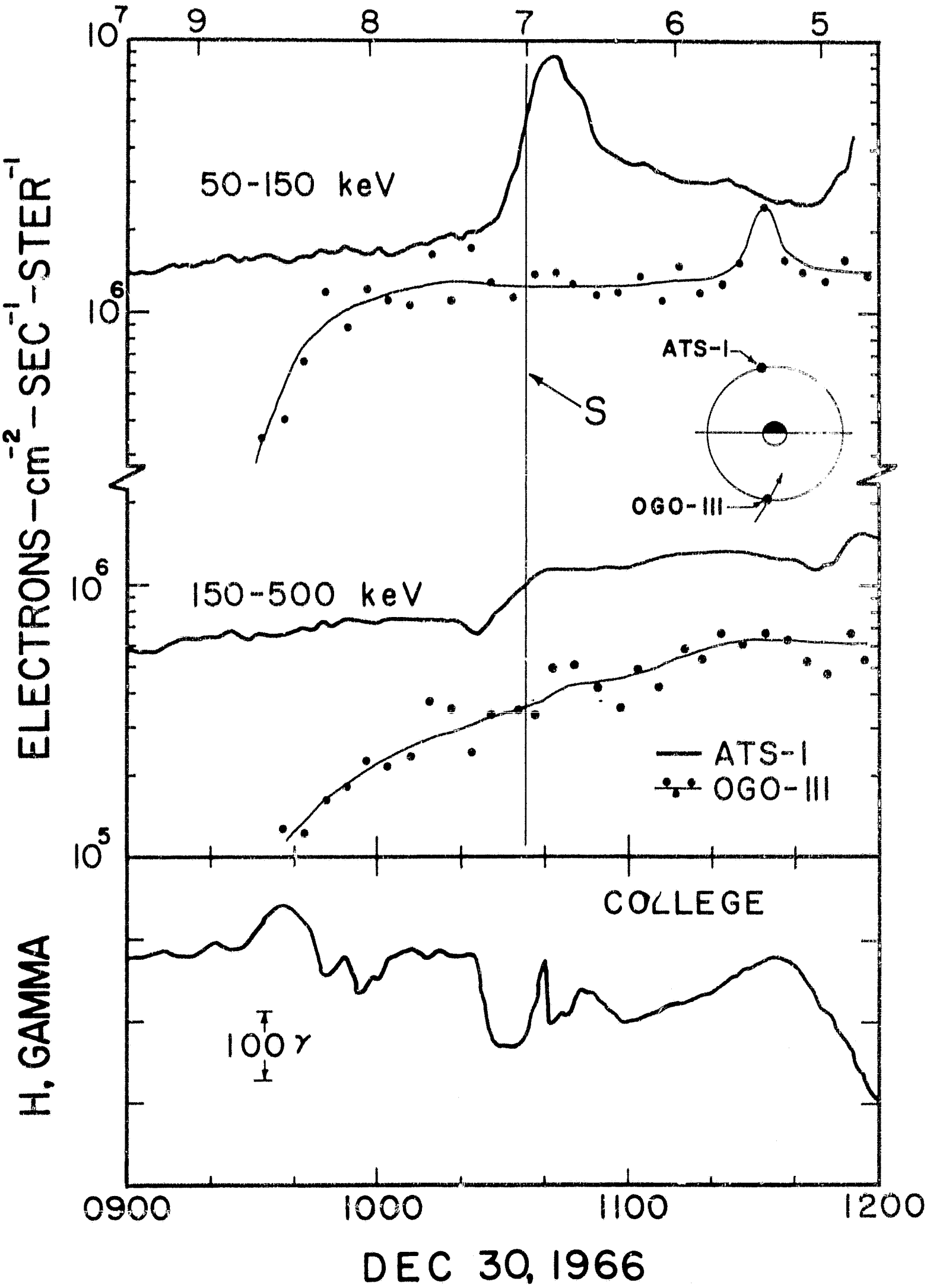
R_E, EARTH RADII
10^7
9
8
7
6
5
50-150 keV
10^6
ATS-I
S
OGO-III
150-500 keV
10^6
ELECTRONS-CM^-2-SEC^-1-STER^-1
ATS-I
OGO-III
10^5
COLLEGE
H, GAMMA
100 γ
0900
1000
1100
1200
DEC 30, 1966

Figure 8

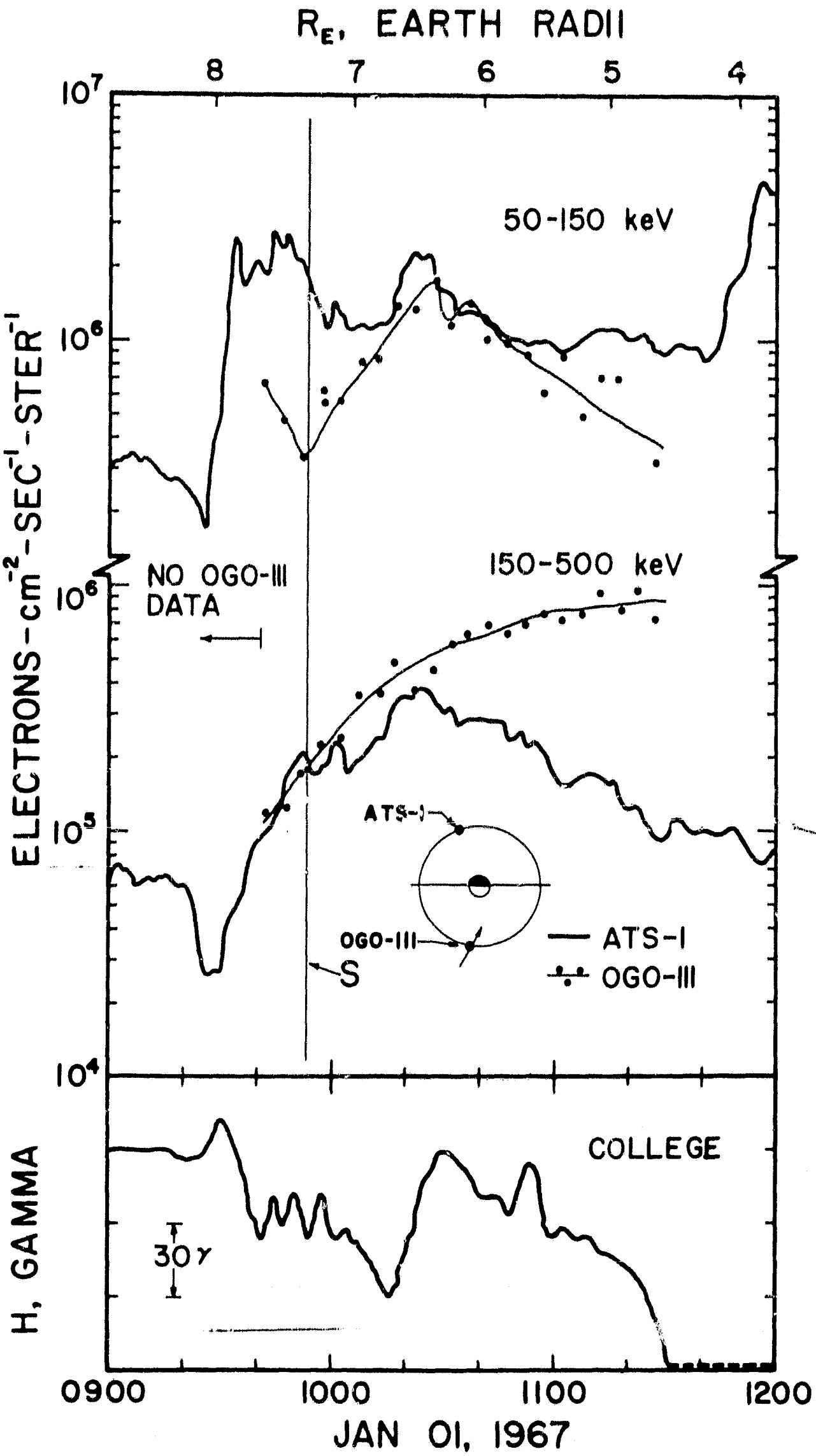
R_E, EARTH RADII
8
7
6
5
4
10^7
10^6
10^5
10^4
50-150 keV
150-500 keV
NO OGO-III DATA
ELECTRONS-cm^-2-SEC^-1-STER^-1
ATS-I
OGO-III
S
ATS-I
OGO-III
H, GAMMA
30γ
COLLEGE
0900
1000
1100
1200
JAN 01, 1967

Figure 9

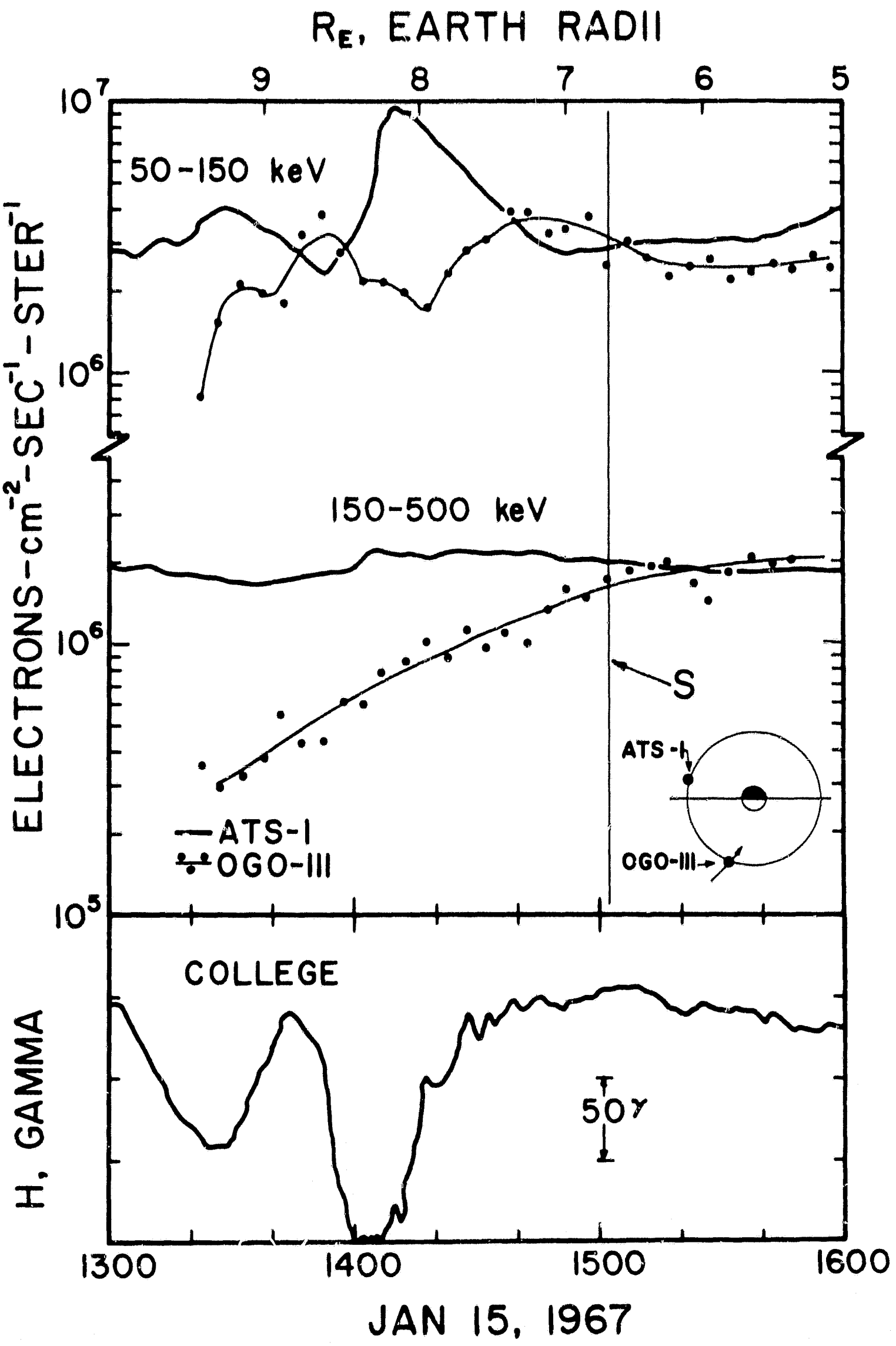
R_E, EARTH RADII
9
8
7
6
5
10^7
50-150 keV
10^6
150-500 keV
10^6
10^5
ELECTRONS-cm^{-2}-SEC^{-1}-STER^{-1}
S
ATS-I
OGO-III
ATS-I
OGO-III
COLLEGE
50γ
H, GAMMA
1300
1400
1500
1600
JAN 15, 1967

Figure 10

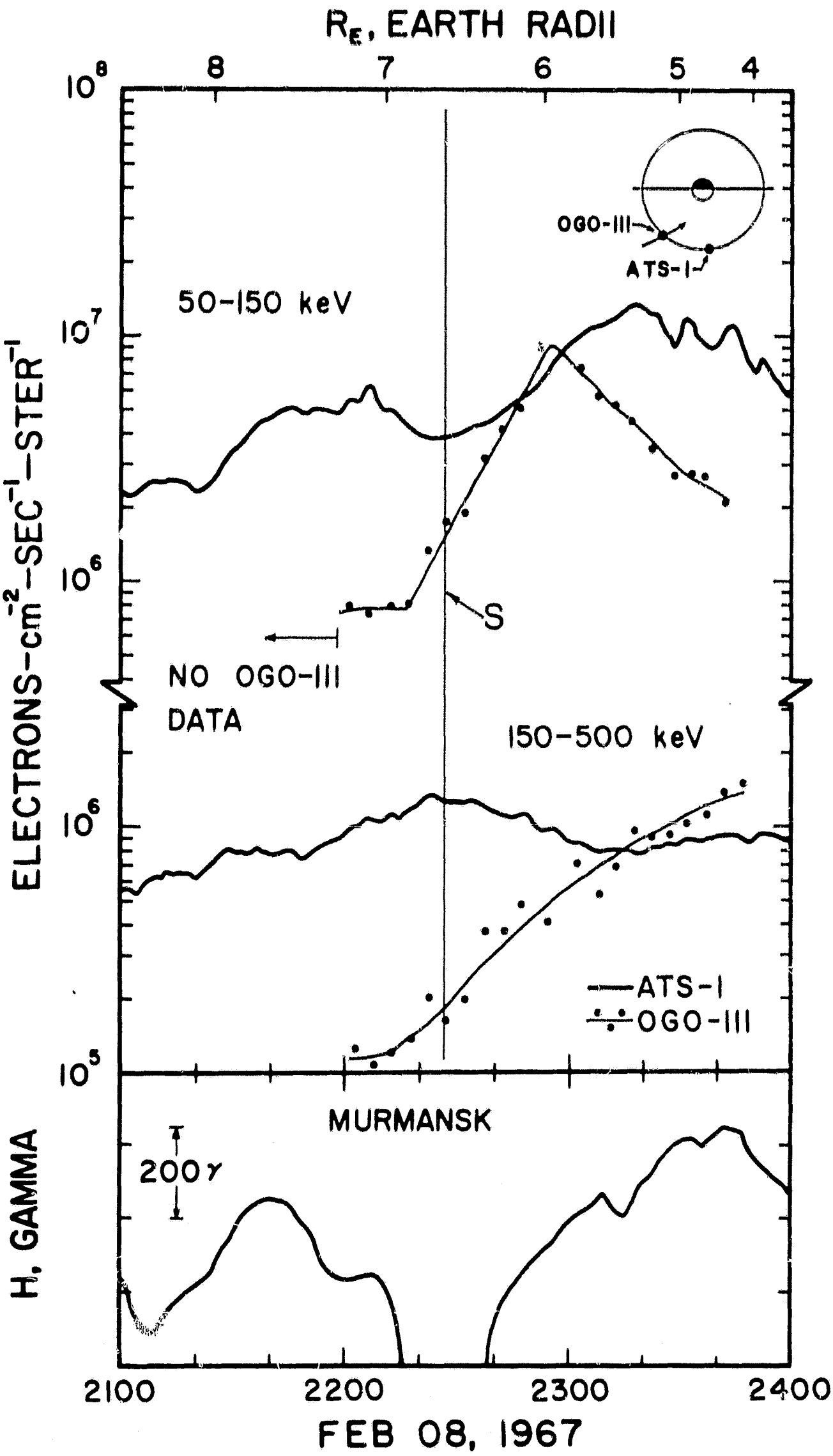
R_E, EARTH RADII
8
7
6
5
4
OGO-III
ATS-I
50-150 keV
NO OGO-III DATA
S
150-500 keV
ATS-I
OGO-III
MURMANSK
200γ
H, GAMMA
ELECTRONS-cm⁻²-SEC⁻¹-STER⁻¹
10⁸
10⁷
10⁶
10⁵
2100
2200
2300
2400
FEB 08, 1967

Figure 11

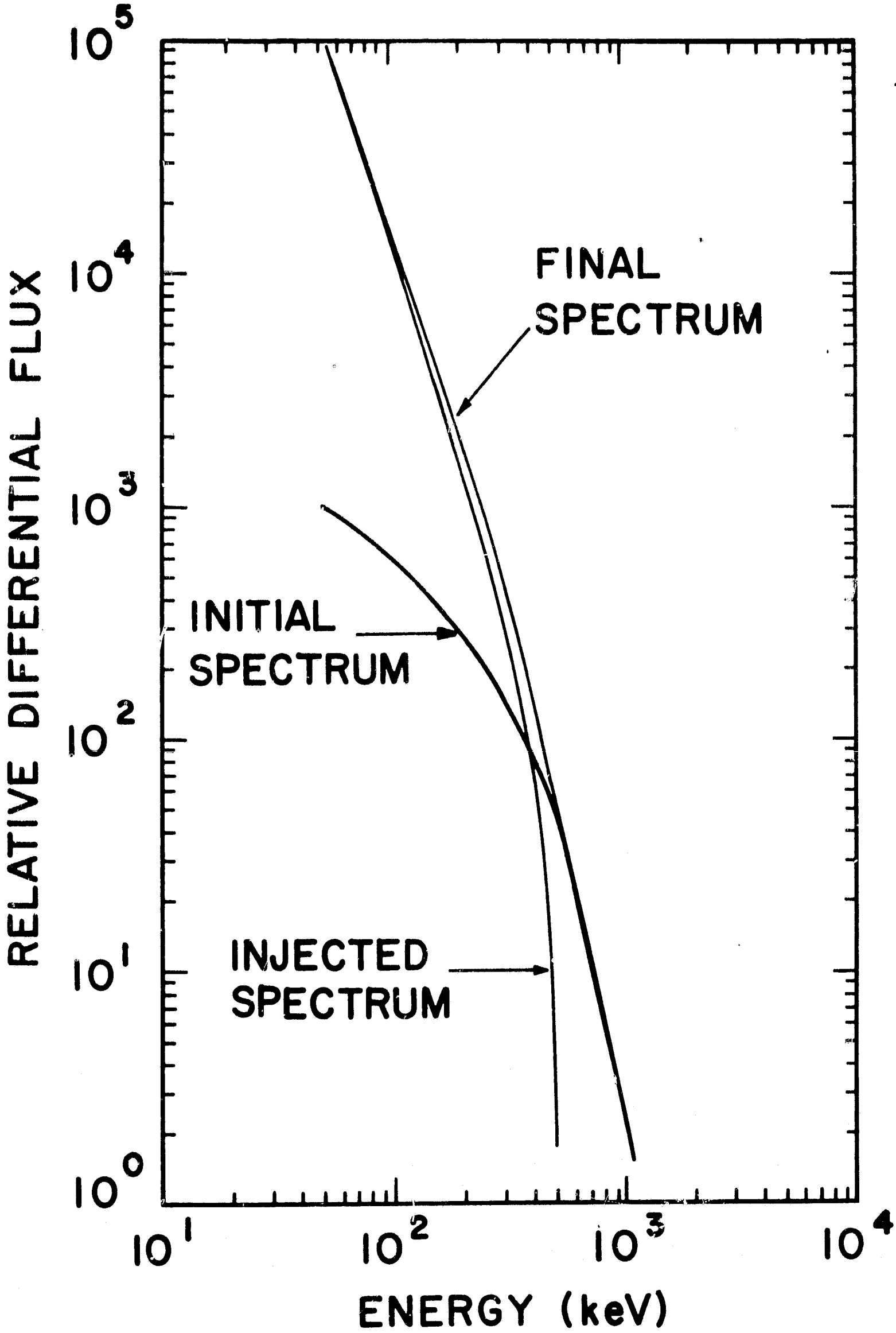
RELATIVE DIFFERENTIAL FLUX
10^5
10^4
10^3
10^2
10^1
10^0
FINAL SPECTRUM
INITIAL SPECTRUM
INJECTED SPECTRUM
10^1
10^2
10^3
10^4
ENERGY (keV)

Figure 12

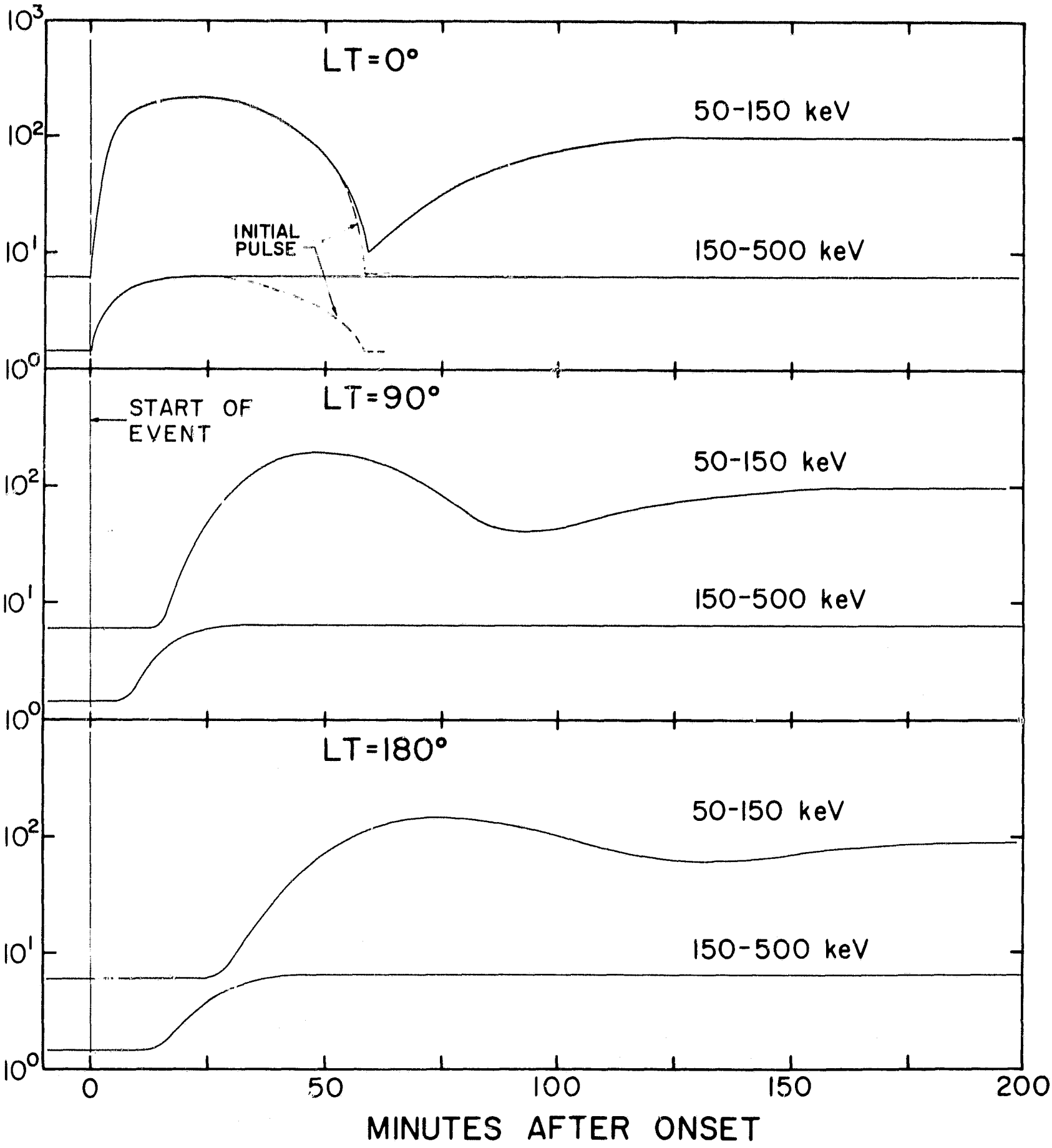
LT=0°
50-150 keV
INITIAL PULSE
150-500 keV
LT=90°
START OF EVENT
50-150 keV
150-500 keV
LT=180°
50-150 keV
150-500 keV
RELATIVE RATE
10^3
10^2
10^1
10^0
0
50
100
150
200
MINUTES AFTER ONSET

Figure 13

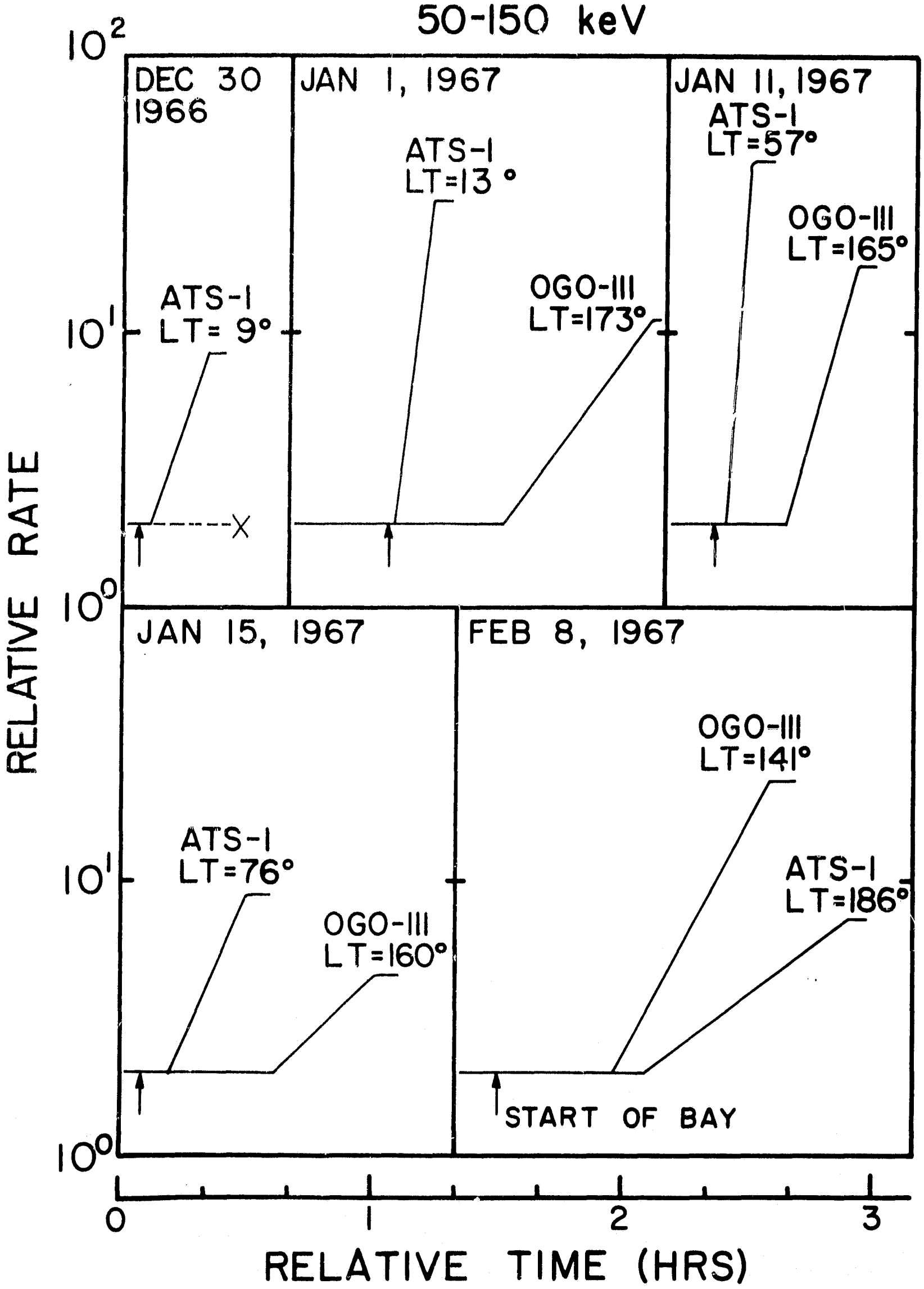
50-150 keV
RELATIVE RATE
10^2
10^1
10^0
DEC 30
1966
ATS-1
LT= 9°
JAN 1, 1967
ATS-1
LT=13°
OGO-III
LT=173°
JAN 11, 1967
ATS-1
LT=57°
OGO-III
LT=165°
JAN 15, 1967
ATS-1
LT=76°
OGO-III
LT=160°
FEB 8, 1967
OGO-III
LT=141°
ATS-1
LT=186°
START OF BAY
0
1
2
3
RELATIVE TIME (HRS)

Figure 14

References

Arnoldy, R. L. and K.-W. Chan, Particle Substorms Observed at the Geostationary Orbit, Transactions of the American Geophysical Union, 50, No. 4, 285 April (1969).

Hess, W. N., The Radiation Belt and Magnetosphere, Blasidell Publishing Co., Waltham, Massachusetts (1968).

Jelly, D. and N. Brice, Changes in Van Allen Radiation Associated with Polar Substorms, J. Geophys. Res., 72, 5919-5931 (1967).

Kane, S. R., K. A. Pfitzer and J. R. Winckler, The Construction, Calibration and Operation of the University of Minnesota Experiments for OGO-I and OGO-III, University of Minnesota Cosmic Ray Technical Report CR-87, September (1966).

Kane, S. R., Application of an Integrating Type Ionization Chamber to Measurements of Radiation in Space. Ph.D. Thesis, University of Minnesota Cosmic Ray Technical Report CR-106, September (1967).

Kennel, C. F. and H. E. Petschek, Limit on Stably Trapped Particle Fluxes, J. Geophys. Res., 71, 1 (1966).

Lezniak, T. W., R. L. Arnoldy, G. K. Parks and J. R. Winckler, Measurement and Intensity of Energetic Electrons at the Equator at 6.6 R_e, Radio Science 3, No. 7, 710-714 (1968) and University of Minnesota Cosmic Ray Technical Report CR-103, June (1967).

Lezniak, T. W. and J. R. Winckler, The Structure of the Magnetopause at 6.6 R_e in Terms of 50-150 keV Electrons, J. Geophys. Res., 73, 5733-5742 (1968) and University of Minnesota Cosmic Ray Technical Report CR-113, September (1967).

Lezniak, T. W. and J. R. Winckler, Magnetospheric Substorm Effects on Energetic Electrons in the Outer Van Allen Belt, University of Minnesota Cosmic Ray

Technical Report CR-137, April (1969). To be published.

McDiarmid, I. B., J. R. Burrows and M. D. Wilson, Morphology of Outer Radiation Zone Electron (E > 35 keV) Acceleration Mechanisms, J. Geophys. Res., 74, 1749-1758 (1969).

Mead, G. D., Deformation of the Geomagnetic Field by the Solar Wind, J. Geophys. Res., 69, 1131-1195 (1964).

Parks, G. K., F. V. Coroniti, R. L. McPherron and K. A. Anderson, Studies of Magnetospheric Substorms, I, Characteristics of Modulated Energetic Electron Precipitation Occurring during Auroral Substorms, J. Geophys. Res., 73, 1685-1696 (1968).

Parks, G. K. and J. R. Winckler, Acceleration of Energetic Electrons Observed at the Synchronous Altitude during Magnetospheric Substorms, J. Geophys. Res., 73, 5786-5791 (1968) and University of Minnesota Cosmic Ray Technical Report CR-120, July (1968).

Pfitzer, K. A. and J. R. Winckler, Experimental Observation of a Large Addition to the Electron Inner Radiation Belt after a Solar Flare Event, J. Geophys. Res., 73, 5792-5797 (1968) and University of Minnesota Cosmic Ray Technical Report CR-121, July (1968).

Pfitzer, K. A., An Experimental Study of Electron Fluxes from 50 keV to 4 meV in the Inner Radiation Belt, Ph.D. Thesis, University of Minnesota Cosmic Ray Technical Report CR-123, August (1968).

Pfitzer, K. A., T. W. Lezniak and J. R. Winckler, Experimental Verification of Drift Shell Splitting in the Distorted Magnetosphere, University of Minnesota Cosmic Ray Technical Report CR-133, April (1969). To be published.

Williams, D. J. and G. D. Mead, Nightside Magnetosphere Configuration as Obtained from Trapped Electrons at 1100 Kilometers, J. Geophys. Res., 70, 3017-3029 (1965).